INTERNATIONAL JOURNAL FOR NUMERICAL METHODS IN FLUIDS, VOL. 6, 409–426 (1986)

TREATMENT OF NON-LINEARITIES IN THE NUMERICAL SOLUTION OF THE INCOMPRESSIBLE NAVIER–STOKES EQUATIONS

P. F. GALPIN AND G. D. RAITHBY

Department of Mechanical Engineering, University of Waterloo, Waterloo, Ontario, Canada N2L 3G1

SUMMARY

The solution of the full non-linear set of discrete fluid flow equations is usually obtained by solving a sequence of linear equations. The type of linearization used can significantly affect the rate of convergence of the sequence to the final solution. The first objective of the present study was to determine the extent to which a full Newton–Raphson linearization of all non-linear terms enhances convergence relative to that obtained using the 'standard' incompressible flow linearization. A direct solution procedure was employed in this evaluation. It was found that the full linearization enhances convergence, especially when grid curvature effects are important.

The direct solution of the linear set is uneconomical. The second objective of the paper was to show how the equations can be effectively solved by an iterative scheme, based on a coupled-equation line solver, which implicitly retains all the inter-equation couplings. This solution method was found to be competitive with the highly refined segregated solution methods that represent the current state-of-the-art.

KEY WORDS Non-linear Newton–Raphson Linearization Incompressible Line Solver

INTRODUCTION

The solutions to complex fluid flow problems are usually obtained by solving the discrete (algebraic) equation analogues of the full equations of motion. Like the underlying differential equations, the discrete equations are non-linear. In order to solve these equations using standard methods the non-linear terms are linearized, the resulting linear equation set is solved, the coefficients are updated, and this 'coefficient update cycle' repeated until the final solution is obtained that satisfies the non-linear equations. This final solution is referred to herein as the 'steady-state solution'.

The rate at which the sequence of solutions to the linear equations converges to the steady-state solution depends in part on the accuracy of the linearization employed.

In compressible flow analysis, a Newton–Raphson linearization of the non-linear terms is often used. Excellent discussions of the linearization, and of the solution of the resulting linear, coupled equation sets, have been provided by Beam and Warming,[1,2] Briley and McDonald[3,4] and MacCormick.[5]

For the limiting case of isothermal and incompressible flow, there are fewer non-linearities in the equations of motion, and those that do appear are usually not subjected to a full Newton–Raphson linearization. As a result of this special treatment, the linear momentum equations become decoupled so that, for a given pressure, each momentum equation can be solved independently from the others. The widely used 'segregated' solution methods[6,7] for incompressible flows depend

0271–2091/86/070409–18$09.00

Received 8 May 1985
Revised 30 August 1985

heavily on this decoupling. Clearly the linearization required to obtain the decoupling is crude, so that more coefficient-update cycles will usually be required to converge to the solution of the non-linear set. The question is, under what conditions do the benefits that accrue from the simple segregated formulation compensate for the increased number of coefficient-update cycles? The purpose of the present paper is to provide evidence relating to this question by addressing two separate smaller, but related issues.

The first issue concerns the effect of linearization on the rate of convergence of the sequence of linear solutions to the steady-state solution. The present paper presents detailed results for two problems, and briefly reports on other problems that have been solved using both the 'standard' linearization, that leads to the segregated equations, and full Newton–Raphson linearization, that leads to fully coupled equations. Since this issue does not involve the solution economy, all solutions were obtained by direct inversion of the full set of linear equations.

The second issue concerns the *cost* of obtaining a solution, to prescribed accuracy, to the non-linear equations. The solution methods employed to solve both the segregated and coupled sets have a major impact on the solution costs and because such methods are constantly being improved, a full evaluation is not possible. Of the available methods for iterative solution of the coupled set,[8,9] the CELS (coupled equation line solver) method of Galpin *et al.*[9] was used.

In the first section of the paper the equations of motion are presented in orthogonal curvilinear co-ordinates, linearization is discussed, and the discrete equations are presented. The next major section describes the direct solution method, and presents results relating to the rate of convergence of the linear-solution sequence.

The second section of the paper extends the CELS method to permit implicit treatment of all inter-equation couplings. The two problems are then re-solved and the solution times to reach a prescribed tolerance are compared to those for the SIMPLEC[7] segregated solution method.

DERIVATION OF THE DISCRETE LINEARIZED EQUATIONS OF MOTION

Differential equations of motion

The governing differential equations of motion for two dimensional, incompressible, isothermal, laminar flow, written in general orthogonal curvilinear co-ordinates are[10]

$$\frac{\partial}{\partial x_1}(\rho h_2 u) + \frac{\partial}{\partial x_2}(\rho h_1 v) = 0, \tag{1}$$

$$\frac{\partial}{\partial t}(\rho u) + \frac{1}{h_1 h_2}\left(\overbrace{\frac{\partial}{\partial x_1}(h_2 \rho u u) + \frac{\partial}{\partial x_2}(h_1 \rho v u)}^{\text{I}} + \overbrace{\rho v u \frac{\partial h_1}{\partial x_2} - \rho v^2 \frac{\partial h_2}{\partial x_1}}^{\text{II}}\right)$$
$$= -\frac{1}{h_1}\frac{\partial p}{\partial x_1} + \frac{1}{h_1 h_2}\left(\frac{\partial}{\partial x_1}(h_2 \sigma_{11}) + \frac{\partial}{\partial x_2}(h_1 \sigma_{21}) + \sigma_{12}\frac{\partial h_1}{\partial x_2} - \sigma_{22}\frac{\partial h_2}{\partial x_1}\right) + \dot{S}_u, \tag{2}$$

$$\frac{\partial}{\partial t}(\rho v) + \frac{1}{h_1 h_2}\left(\overbrace{\frac{\partial}{\partial x_1}(h_2 \rho u v) + \frac{\partial}{\partial x_2}(h_1 \rho v v)}^{\text{I}} + \overbrace{\rho u v \frac{\partial h_2}{\partial x_1} - \rho u^2 \frac{\partial h_1}{\partial x_2}}^{\text{II}}\right)$$
$$= -\frac{1}{h_2}\frac{\partial p}{\partial x_2} + \frac{1}{h_1 h_2}\left(\frac{\partial}{\partial x_1}(h_2 \sigma_{12}) + \frac{\partial}{\partial x_2}(h_1 \sigma_{22}) + \sigma_{21}\frac{\partial h_2}{\partial x_1} - \sigma_{11}\frac{\partial h_1}{\partial x_2}\right) + \dot{S}_v. \tag{3}$$

The stresses, σ, are related to the velocities via the following relations for a Newtonian fluid:

$$\sigma_{11} = 2\mu\left[\frac{1}{h_1}\frac{\partial u}{\partial x_1} + \frac{v}{h_1 h_2}\frac{\partial h_1}{\partial x_2}\right], \quad \sigma_{22} = 2\mu\left[\frac{1}{h_2}\frac{\partial v}{\partial x_2} + \frac{u}{h_1 h_2}\frac{\partial h_2}{\partial x_1}\right],$$

$$\sigma_{12} = \sigma_{21} = \left[\frac{h_2}{h_1}\frac{\partial}{\partial x_1}\left(\frac{v}{h_2}\right) + \frac{h_1}{h_2}\frac{\partial}{\partial x_2}\left(\frac{u}{h_1}\right)\right]. \tag{4}$$

In these equations u and v are the velocity components in the x_1- and x_2-directions, respectively, and h_1 and h_2 are the metrics in these directions. Other variables are defined in the Nomenclature section.

Examination of equations (1)–(4) reveals several linear and non-linear inter-equation couplings. The linear continuity equation imposes a strong pressure-velocity coupling (p–V coupling). Substitution of the stresses into the momentum equations result in an apparently strong inter-momentum equation coupling, but application of mass conservation eliminates this coupling almost entirely. The advection terms, denoted by I in equations (2) and (3), and acceleration terms, denoted by II, are non-linear and impose additional intra- and inter-momentum equation couplings.

Discrete equations of motion

To derive the discrete equations of motion the solution domain is first subdivided into orthogonal control volumes. Pressure nodes are located at the centres of these volumes, as shown in Figure 1. Velocity nodes (Figures 1 and 2) are located in velocity control volumes which are staggered between the pressure nodes, as originally proposed by Harlow and Welch.[11] The derivation of the algebraic equations for mass and momentum is now outlined, focusing on the treatment of the non-linear terms; details of the term-by-term integrations are found elsewhere.[12]

Discrete continuity equation. The differential continuity equation is integrated over a pressure control volume to obtain a discrete continuity equation. This algebraic equation is linear, for

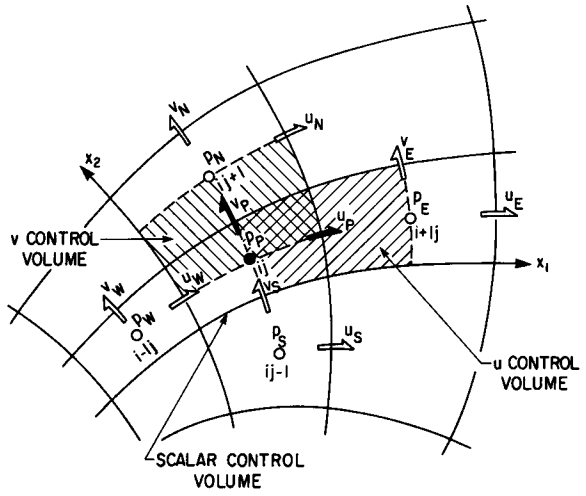

Figure 1. General orthogonal grid layout showing the location of various dependent variables around a pressure (continuity) control volume

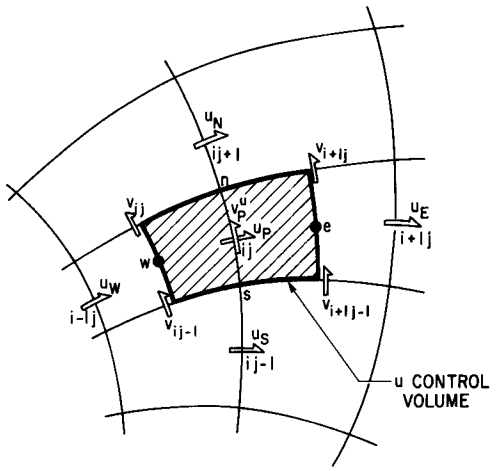

Figure 2. General orthogonal grid layout showing the location of the nodal point and the face-point velocities around a u-momentum control volume

incompressible flow, and can be immediately written in terms of nodal velocities (Figure 1) as

$$A_E^{c,u}u_P + A_W^{c,u}u_W + A_N^{c,v}v_P + A_S^{c,v}v_S = 0, \tag{5}$$

where $A_E^{c,u}u_P$, for example, represents the mass flow leaving the control volume through its east face.

Discrete momentum equations. Integration of the u-momentum equation over its control volume is simplified by the stress-flux formulation[12] where the stresses are divided into active and lagged (previous time level) components. Term-by-term integration then gives an implicit discrete u-momentum equation in terms of nodal point variables (indicated with upper case subscripts) and face point variables (values at faces of the control volume indicated with lower case subscripts, Figure 2) of the form

$$\begin{aligned}
&\underset{\text{Ia}}{\frac{M}{\Delta t}(u_P - u_P^0)} + \underset{\text{Ib}}{\rho A_e u_e u_e} - \underset{\text{IIa}}{\rho A_w u_w u_w} + \underset{\text{IIb}}{\rho A_n v_n u_n} - \underset{\text{IIIa}}{\rho A_s v_s u_s} + \underset{\text{IIIb}}{\rho(A_n - A_s)u_P v_P^u} - \rho(A_e - A_w)v_P^u v_P^u \\
&= \mu\frac{A_e}{\Delta S_{1e}}(u_E - u_P) - \mu\frac{A_w}{\Delta S_{1w}}(u_P - u_W) + \mu\frac{A_n}{\Delta S_{2n}}(u_N - u_P) - \mu\frac{A_s}{\Delta S_{2s}}(u_P - u_S) \\
&\quad - \frac{\text{Vol}}{\Delta S_{1P}}(p_E - p_P) + B^u,
\end{aligned} \tag{6}$$

Terms I–III contain non-linear products of u and v. Terms I–II are the 'advection' terms, and terms III are the 'acceleration' terms that vanish when the control volumes become Cartesian.

To obtain the final form of the discrete linear u-momentum equation, all non-linear terms must be linearized and all face point velocities must be approximated in terms of nodal velocities. Two possible linearizations are examined, followed by brief discussions of the discretization and relaxation schemes used here. In the discussions that follow, variables denoted by superscript 0 are evaluated at t^0, the solution from the most recent time level or coefficient update iteration. Such variables are referred to as 'fixed' or 'lagged'. Variables without this superscript are evaluated at the $t^0 + \Delta t$ time level, and are therefore referred to as 'active'.

(i) Standard linearization: the 'standard' incompressible flow linearization fixes one or both velocities in each product. In the advection terms, the velocities associated with the mass flow (or the 'advecting' velocity u in Term I and v in Term II) are fixed while the other ('advected') velocity in each product is kept active. Acceleration term IIIa is linearized by fixing both u_P and v_P^u, or by fixing v_P^u only, whereas both v_P^u velocities are fixed in term IIIb. As discussed earlier, these linearizations uncouple the u-momentum equation from the v-momentum equation. If the v-momentum equation is linearized in a similar fashion, the resulting uncoupled momentum equation (UME) set is indirectly coupled only through pressure.

(ii) Newton–Raphson linearization: the momentum equations are more directly coupled when a Newton–Raphson linearization of all non-linear terms is used (i.e. a Taylor series expansion that ignores terms beyond first order). A classical Newton–Raphson linearization of the non-linear product uv, for example, is

$$\begin{aligned} uv &\approx u^0v^0 + \frac{\partial}{\partial u}(uv)^0(u-u^0) + \frac{\partial}{\partial v}(uv)^0(v-v^0) \\ &= v^0u + u^0v - u^0v^0. \end{aligned} \tag{7a}$$

The leading term, v^0u, is recognized as the standard linearization described above.

All of the non-linear terms in equation (6) can be linearized in the manner demonstrated in equation (7a), but care must be taken in anticipation of the eventual use of iterative linear solution methods. In particular, the introduction of negative coefficients in the linear algebraic momentum equations should be avoided and the diagonal dominance of each linear equation should be preserved, to ensure rapid convergence of iterative solvers. For example, for the u-momentum equation special consideration must be given when linearizing terms I and IIIa.

Consider the classical Newton–Raphson linearization of term Ia, written to emphasize the different roles of the advecting and advected velocities as

$$\rho A u_e u_e = (\rho A u_e) u_e = \dot{m}_e u_e \approx \dot{m}_e^0 u_e + \dot{m}_e u_e^0 - \dot{m}_e^0 u_e^0. \tag{7b}$$

In the present application, $\dot{m}_e$ is calculated as the average of the mass flows through the adjacent faces of the scalar control volumes

$$\dot{m}_e = \tfrac{1}{2}\rho(A_E u_E + A_W u_P), \tag{7c}$$

where, for example, A_E is the area of the east face of the scalar control volume. Such an evaluation ensures that mass is conserved over the u-control volume, but implies that the advecting and advected velocities are different. If equation (7c) is substituted into equation (7b), large negative coefficients may result. This situation is avoided by *assuming*, for the purposes of the linearization only, that the advected and advecting velocities are equal, so that

$$\dot{m}_e u_e \approx 2\dot{m}_e^0 u_e - \dot{m}_e^0 u_e^0. \tag{7d}$$

This requirement is then dropped when $\dot{m}_e$ and u_e are evaluated. Although this practice ensures that no negative coefficients are introduced, the linearization is no longer truly second order accurate. Similar considerations apply to term Ib.

Care is also taken in the Newton–Raphson linearization of term IIIa to ensure that the term's contribution to the total coefficient on u_P increases the diagonal dominance of the linear equation.

(iii) Face point velocity approximations: independent of which of the standard or Newton–Raphson linearization are employed, the face point velocities must be approximated in terms of the nodal velocities. In this work, the advected velocities were approximated by a simple upstream weighted scheme.[13] The results and conclusions of the present work, however, apply in principle to higher spatially accurate discretization schemes.

(iv) Relaxation: rather than follow a transient evolution, a distorted transient (or iterative) method was employed which introduced the relaxation parameter E[7,14] into the terms in equation (6) which contain Δt, by making the replacement

$$\Delta t = E\Delta t_{\max},$$

where $\Delta t_{\max}$ is the maximum time step allowable if the simplest explicit transient solution method were to be used to integrate the time-dependent momentum equations. The physical interpretation and advantages of the E-factor formulation are presented elsewhere.[7] It is sufficient to note here that such relaxation is often required to accelerate convergence, or prevent divergence, of the coefficient-update cycle, and that E-values significantly in excess of unity are required to justify the increased overhead incurred when solving the algebraic momentum equations by implicit, rather than explicit methods.

(v) Final discrete linear momentum equations: when the Newton–Raphson linearizations above are employed, together with the noted discretization scheme and relaxation, the final form of the discrete linear u-momentum equation is

$$A_P^{u,u}u_{ij} = A_E^{u,u}u_{i+1j} + A_W^{u,u}u_{i-1j} + A_N^{u,u}u_{ij+1} + A_S^{u,u}u_{ij-1} + A_{NE}^{u,v}v_{i+1j} + A_{NW}^{u,v}v_{ij} + A_{SE}^{u,v}v_{i+1j-1} + A_{SW}^{u,v}v_{ij-1} + A_E^{u,p}p_{i+1j} + A_W^{u,p}p_{ij} + B^{*u}. \quad (8)$$

The locations of the nodal point variables are shown in Figure 2, and the coefficients are presented in the Appendix.

The discrete v-momentum equation is obtained by employing similar approximations and Newton–Raphson linearization of all its non-linear terms, as discussed for the u-momentum equation, and is of the form

$$A_P^{v,v}v_{ij} = A_E^{v,v}v_{i+1j} + A_W^{v,v}v_{i-1j} + A_N^{v,v}v_{ij+1} + A_S^{v,v}v_{ij-1} + A_{NE}^{v,u}u_{ij+1} + A_{NW}^{v,u}u_{i-1j+1} + A_{SE}^{v,u}u_{ij} + A_{SW}^{v,u}u_{i-1j} + A_N^{v,p}p_{ij+1} + A_S^{v,p}p_{ij} + B^{*v}. \quad (9)$$

Equations (8) and (9) form a coupled momentum equation (CME) set that possess direct inter-momentum equation couplings through the $A^{u,v}$ and $A^{v,u}$ coefficients. The CME set cannot be solved in a segregated manner.

EFFECT OF LINEARIZATION ON CONVERGENCE TO THE NON-LINEAR SOLUTION

The linear equation set is comprised of one continuity equation, like equation (5), for each pressure control volume, and one u- and v-momentum equation, like equations (8) and (9), for each u- and v-control volume, respectively. The formation of the coefficients together with the solution of this set comprises one coefficient update cycle. As described in the Introduction, the purpose of this section is to establish the effect of linearization on the convergence of the coefficient update cycle. In this section each solution to the linear set was obtained by direct solution of the full equation set.

Direct solution of linear equation set

The direct linear solution is implemented by first transforming each continuity equation into an equation for pressure. Following the procedure of Zedan and Schneider,[15] the velocities in the continuity equation (5) are replaced by their respective momentum equations (8) and (9), thereby

forming a diagonally dominant pressure equation of the form

$$A_P^{p,p} p_{ij} = \sum A_{nb}^{p,p} p_{nb} + \sum A_{nb}^{p,u} u_{nb} + \sum A_{nb}^{p,v} v_{nb} + B^p, \tag{10}$$

where p_{ij} is expressed in terms of its four pressure, eight u-velocity and eight v-velocity neighbours.

The fully coupled linear equation set, equations (8)–(10), is solved directly to give the nodal values of u, v and p, using an LU decomposition algorithm. Both the CME and the UME sets were solved in this manner by supplying the appropriate linear equation coefficients to the direct solver.

Test problems and procedure

Several flows have been calculated using this direct solver. Only two representative test flows are present here: flow of air over a rearward facing step discretized using a 27 × 17 Cartesian grid (Figure 3A), and a similar flow on a 27 × 17 curvilinear grid (Figure 4A). These are referred to hereafter as the Cartesian and curvilinear test problems, respectively. The computed flow fields for these problems are presented in Figures 3B and 4B.

The steady-state predictions of each of the test problems were determined by repeating the coefficient update cycle until changes in the dependent variables between successive linear solutions were of the order of machine zero. These steady-state solutions are referred to as 'exact' solutions and are, to machine accuracy, the same, independent of whether the UME or CME set is employed.

The problems are then re-solved, with all variables initialized to zero, using both the UME and the CME sets. The r.m.s. error of all variables from the exact solution, ε_{rms}, is determined after each

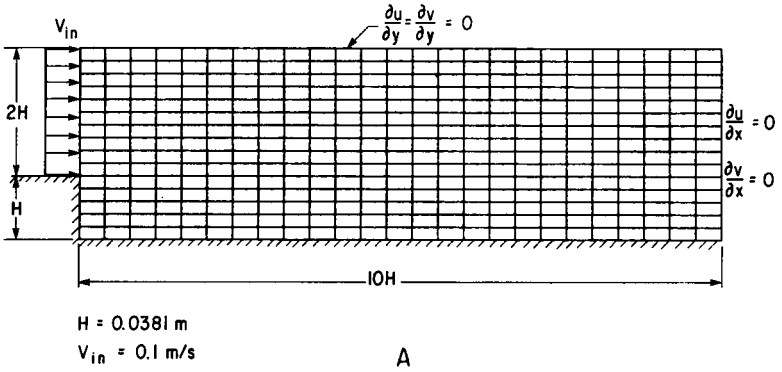

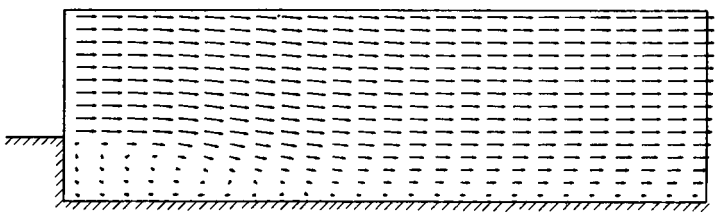

Figure 3. Grid and boundary conditions for the Cartesian test problem (A), and the calculated velocity vectors for air flowing over the step (B)

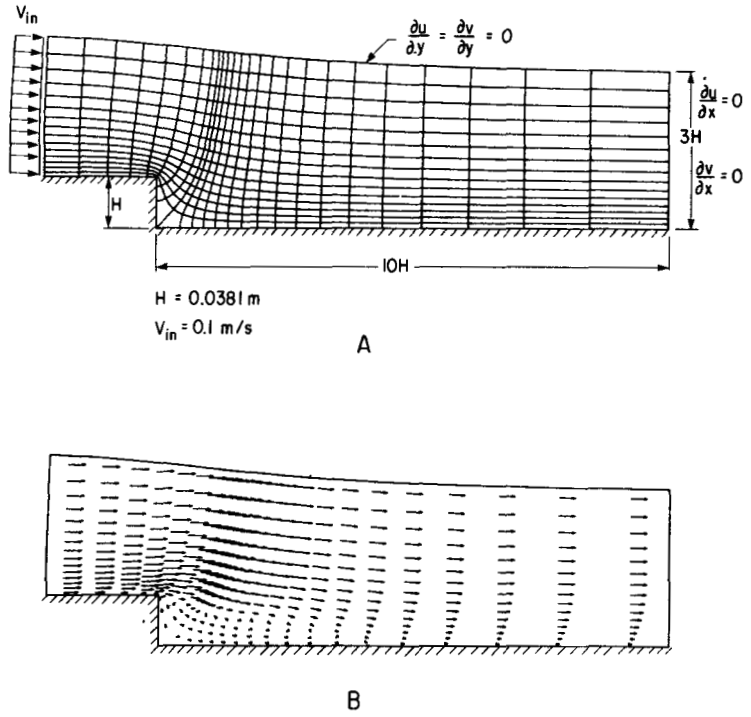

Figure 4. Grid and boundary conditions for the curvilinear test problem (A), and the calculated velocity vectors for air flowing over the step (B)

coefficient update cycle. Typically the pressure solution is more sensitive to change than the velocity solution, and the r.m.s. error of pressure from the exact solution, ε^p_{rms}, is a sensitive indicator of convergence. The values of ε^p_{rms} plotted as a function of the count on the coefficient update cycle provide a qualitative illustration of the convergence behaviour for each linearization method.

To provide a single number to characterize the convergence rate, the number of coefficient updates required to compute all variables to within ε_{max} of their exact values are also reported. Here ε_{max} is defined as the maximum deviation of the dependent variables from their steady values normalized by the steady-state range of each variable. A value of $\varepsilon_{max} = 10^{-3}$ was specified for both the test problems. At this tolerance calculated variables are well above machine round-off, but the tolerance is sufficient to demonstrate the convergence behaviour.

Results

Cartesian test problem. Qualitatively the solution convergence behaviour observed for the Cartesian test problem, independent of the linearization used and of the degree of relaxation, is smooth and monotonic (Figure 5A). The difference in convergence rates observed when solving the CME and UME sets is small during the initial coefficient updates. As the steady-state solution is approached, however, the convergence rate attained solving the CME set becomes marginally faster than that for the UME set.

The number of coefficient updates required to compute all variables to within ε_{max} of the exact solution are plotted in Figure 5B as a function of the relaxation, E. The CME set is seen to converge

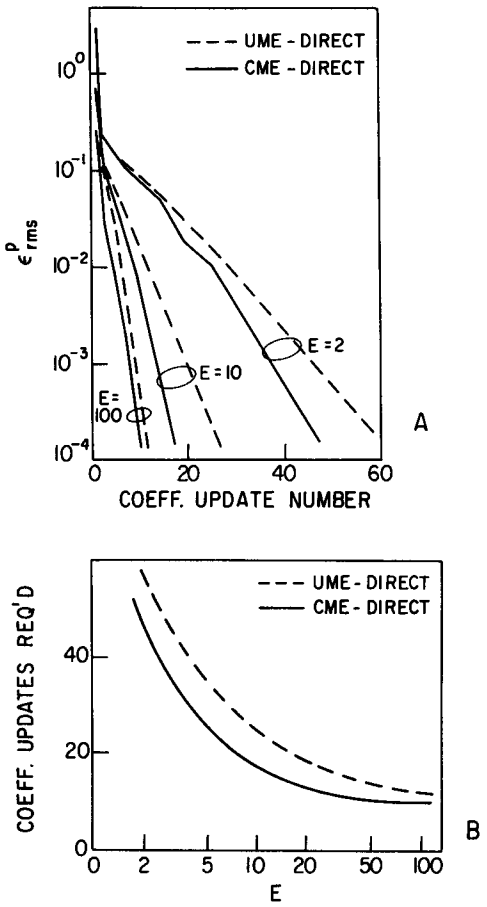

Figure 5. RMS error in the pressure solution, ε^p_{rms}, versus the coefficient update number (A), and the total number of coefficient updates required for all variables to converge within $\varepsilon_{max} = 10^{-3}$ of their exact values versus the relaxation, E (B), comparing the UME and CME sets solved directly for the Cartesian test problem

only marginally faster than the UME set for all values of E, the largest difference occurring at intermediate values of E. The Newton–Raphson linearization of the non-linear terms in the Cartesian momentum equations (the advection terms) thus does not significantly accelerate or improve convergence of the coefficient update cycle. This has been observed for several other Cartesian test problems as well.

Curvilinear test problem. The convergence behaviour of the curvilinear test problem is illustrated in Figure 6A. For $E = 2$, both the CME and the UME sets converge smoothly and monotonically. For $E = 10$, both sets converge equally well up to the 13th coefficient update, after which the UME set wanders slightly and converges at a slower rate. For $E = 100$, the CME set is notably faster and more stable than the UME set, resulting in a significant reduction in the number of coefficient updates required.

Figure 6B reveals that the CME set requires consistently fewer coefficient updates to converge to within ε_{max} than the UME set, and that the CME set is less sensitive to the value of E. The convergence rate is optimal at $E \approx 10$, degrading for both methods for all other values of E, a

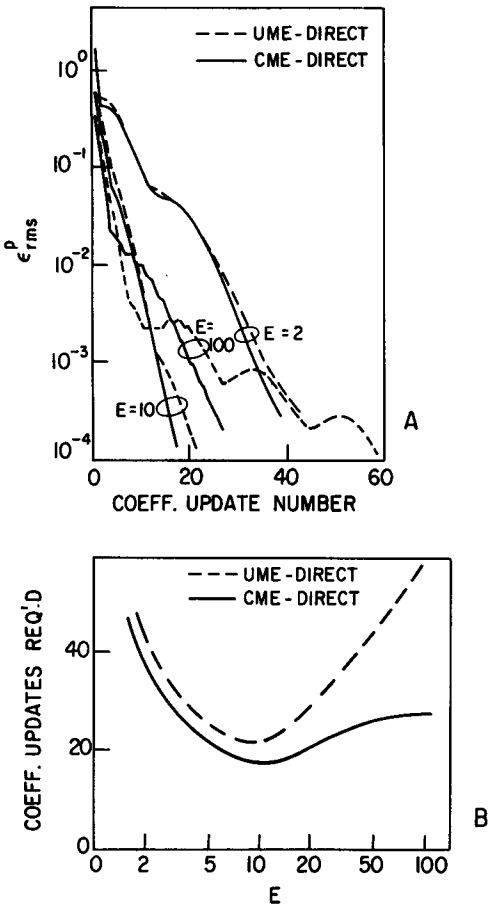

Figure 6. RMS error in the pressure solution, ε^p_{rms}, versus the coefficient update number (A), and the total number of coefficient updates required for all variables to converge within $\varepsilon_{max} = 10^{-3}$ of their exact values versus the relaxation, E (B), comparing the UME and CME sets solved directly for the curvilinear test problem

behaviour not observed for the Cartesian test problem. Couplings exist between the curvilinear momentum equations through the acceleration terms, as well as the advection terms, for this flow and grid. The Newton–Raphson linearization of these terms is responsible for the improved convergence behaviour of the CME set, as each linear solution accounts implicitly for the inter-momentum equation couplings. The convergence behaviour of the curvilinear problem thus depends strongly both on the method of linearization and on the degree of relaxation used.

Note on consistency. Although not presented, similar calculations were made for these and other test problems employing a Newton–Raphson linearization only for selected non-linear terms (e.g. only for advection term Ia, or only for acceleration term IIIb). The convergence behaviour was often much worse than for the case where all non-linear terms were linearized in the usual approach, and was never as good as the case where all non-linear terms were represented by a Newton–Raphson linearization. Further tests of inconsistent term-by-term linearizations were thus abandoned.

Note on the early stages of the solution. It has been observed for a few test problems, not presented here, that solving the fully linearized momentum equation set gives poor performance during the very early stages of the solution. This is not surprising, as the Newton–Raphson linearization is strictly valid only when the solution is 'near' the correct solution. All flows computed to date using the fully linearized momentum equations were started with the solution fields set to zero in order to allow for a clear comparison of methods. However, it would be more desirable, in general, to solve using the 'standard' incompressible flow linearizations until the gross features of the flow are established (i.e. for the first 3–5 coefficient update cycles, starting from zero fields), and then solve using the full linearizations to accelerate convergence.

Note on order of convergence. The solution of the CME set for the two problems just considered, as well as for several other problems studied, leads to linear convergence. Ideally a Newton–Raphson linearization would lead to quadratic convergence. Quadratic convergence is in fact obtained if equations such as (7b) are used, if there is no under-relaxation ($E = \infty$), and if the factors associated with upstream weighting are either specified constants or are included in the Newton–Raphson linearization. These algebraic equations are, however, ill suited for iterative solution methods, and were not considered further.

Summary of direct solution results

Based on the results of these and other test problems, the Newton–Raphson linearization of the non-linear terms in the momentum equations is desirable in that: (1) convergence is smooth and monotonic, (2) convergence is accelerated for all values of E and (3) the convergence rate is less sensitive to the relaxation used (i.e. the value of E used). Further, it was found that the linearizations used in each equation must be consistent on a term-by-term basis. The direct solver results justify an investigation of the application of an iterative *linear* solver for the CME set, focusing on the possibility of reducing the total computational effort.

ITERATIVE SOLUTION OF THE COUPLED EQUATIONS

Iterative solution method

An iterative method based on a coupled equation line solver (CELS) was presented previously for the solution of the UME set. Comparisons with state-of-the-art segregated methods (e.g. SIMPLER[6] and SIMPLEC[7] indicated that CELS was competitive in terms of both computational effort and simplicity. The CELS method implicitly treats the p–V coupling so that solutions to the linear set are obtained for a very wide range of E-values.

The CELS solution method can be easily extended to account for coupled momentum equations, making it an attractive solver for the CME set. Attention is now turned to this derivation.

The CELS solution method. The CELS solution method simultaneously solves the momentum and continuity equations along a 'line' of control volumes. The values of u, v and p are improved by successively solving line-by-line in each co-ordinate direction over the entire domain (sweeping) until the desired degree of satisfaction of the linear equation set is obtained.

As in the original derivation of CELS, the variables behind and ahead of the current line are fixed at their most recent estimates (from the previous sweep). Along a line of constant j equations (5), (8)

and (9) become

$$A_P^{u,u}u_i = A_E^{u,u}u_{i+1} + A_W^{u,u}u_{i-1} + A_{NE}^{u,v}v_{i+1} + A_{NW}^{u,v}v_i + A_E^{u,p}p_{i+1} + A_W^{u,p}p_i + b^u, \tag{11}$$

$$A_P^{v,v}v_i = A_E^{v,v}v_{i+1} + A_W^{v,v}v_{i-1} + A_{SE}^{v,u}u_i + A_{SW}^{v,u}u_{i-1} + A_S^{v,p}p_i + b^v, \tag{12}$$

$$0 = A_E^{c,u}u_i + A_W^{c,u}u_{i-1} + A_N^{c,v}v_i + b^c, \tag{13}$$

where the new source terms are

$$b^u = B^u + A_N^{u,u}u_{ij+1}^* + A_S^{u,u}u_{ij-1}^* + A_{SE}^{u,v}v_{i+1j-1}^* + A_{SW}^{u,v}v_{ij-1}^*, \tag{11a}$$

$$b^v = B^v + A_N^{v,v}v_{ij+1}^* + A_S^{v,v}v_{ij-1}^* + A_{NE}^{v,u}u_{ij+1}^* + A_{NW}^{v,u}u_{i-1j+1}^* + A_N^{v,p}p_{ij+1}^*, \tag{12a}$$

$$b^c = A_S^{c,v}v_{ij-1}^*. \tag{13a}$$

The subscript j is implied on all terms and variables if it does not appear explicitly, and superscript * denotes the most recent estimate.

The v-momentum equation (12), is rearranged into a derived equation for p_i in terms of u-velocities by making three substitutions of the continuity equation (13), to eliminate the v-velocities. The v-velocities in the u-momentum equation (11), are also eliminated using continuity, and finally the pressures p_{i+1} and p_i are eliminated from this u-momentum equation using the derived pressure equation. The resulting penta-diagonal equation for u_i is efficiently solved using a penta-diagonal solution algorithm.[9] The pressures and v-velocities can then be immediately calculated, yielding the exact simultaneous solution of equations (11)–(13).

The following recommendations[9] were also used to enhance the convergence of CELS: block pressure correction was used after each sweep, relaxation was introduced within the linear solver and a residual reduction criterion was used to terminate the sweep cycle.

The above proposed extension of CELS to incorporate the CME set was verified by repeating the calculations of several test problems. A tight residual reduction criterion was enforced for each solution of the linear equation set, solving each essentially to machine round-off. The numerical results compared exactly (to round-off) to those obtained when each linear set was solved directly.

If the residual reduction criterion is now made much smaller, the computational effort expended on each linear equation set reduces drastically at the possible expense of requiring additional coefficient updates to converge to the steady-state. The total computational effort to solve the non-linear equations can be minimized in this manner; the minimum computational effort for the two test problems is given below.

Test problems revisited

The flows for the Cartesian and curvilinear test problems described earlier were recalculated, comparing the relative performance of the CELS method applied to the CME coefficients (CELS-CME), the CELS method applied to the UME coefficients (CELS-UME) and the SIMPLEC method[7] (implemented in the recommended method whereby only one SIMPLEC iteration is performed for each new set of coefficients). For each of the three solution methods, the parameters associated with the iterative update of the linear equations were determined so as to minimize the computational effort at each method's optimal value of E. The numerical experiments used to determine these parameters demonstrated that all three methods were about equally sensitive to departures from their optimal values.

The sensitivity of the total computational effort, however, is a strong function of the major relaxation factor, E, for all of the methods. The solution convergence rate is thus illustrated by plotting the total number of coefficient updates required to obtain convergence of all variables to

ε_{max}, and the total computational effort to reach this convergence, as a function of E. For these tests, a value of $\varepsilon_{max} = 10^{-4}$ was used. All computational times refer to calculations on a VAX 780 (no floating point accelerator) running VMS-FORTRAN.

Cartesian test problem. The convergence behaviour of the Cartesian test problem depends strongly on the solution method and on the relaxation, E (Figure 7). At small E, all three methods require approximately the same number of coefficient updates to satisfy the convergence criterion, ε_{max} (Figure 7A). For values of E in excess of 4, SIMPLEC experiences a sharp increase in the number of coefficient updates due to the poor treatment of the p–V coupling, whereas the CME-CELS and UME-CELS methods continue to converge rapidly. At this same value of E, the CME-CELS method begins to converge marginally faster than the UME-CELS method, owing to the improved treatment of the non-linear terms in the momentum equations. As a further indicator of the performance of CME-CELS, it is interesting to compare its convergence behaviour (requiring an average 7·8 cpu seconds per coefficient update) to the convergence behaviour of the direct linear solution of the CME set, the dashed line denoted CME-direct in Figure 7A (requiring an average 243 cpu seconds per coefficient update).

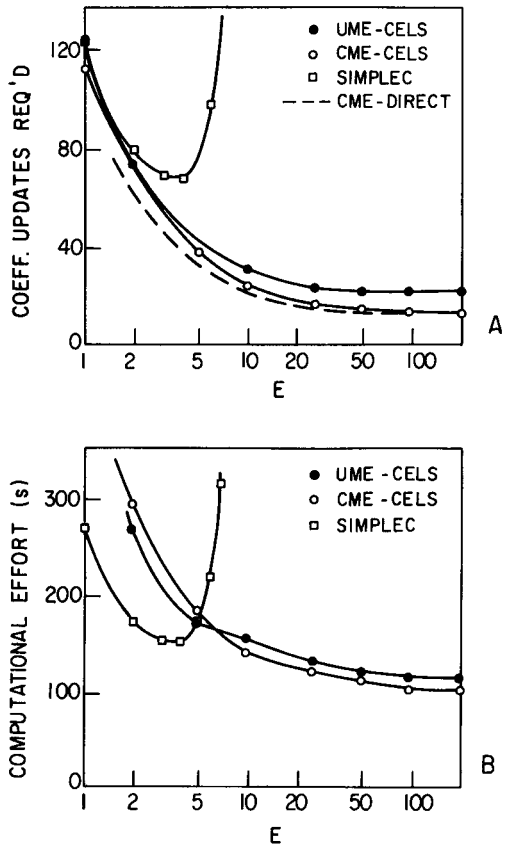

Figure 7. Convergence behaviour of the Cartesian test problem for various solution methods, measured in terms of the number of coefficient updates required (A), and the total computational effort required (B) for all variables to converge within $\varepsilon_{max} = 10^{-4}$ of their exact values versus the relaxation, E

The minimum computational effort required by each of the three methods is of the same order, with SIMPLEC requiring the greatest computational effort and CME-CELS the least effort (Figure 7B).

Curvilinear test problem. The convergence behaviour of the curvilinear test problem is similar to that of the Cartesian test problem, only now the differences between the three methods are exaggerated (Figure 8). The p–V coupling breakdown occurs at a lower value of E (Figure 8A) for SIMPLEC, possibly aggravated by the poor linearization of the acceleration terms in this method. The CME-CELS and UME-CELS methods perform similarly for $E < 5$. For $E > 5$, the UME-CELS method behaves poorly compared to CME-CELS. Clearly the Newton–Raphson treatment of the non-linear acceleration terms in this instance accelerate and stabilize convergence. For comparison purposes, the CME-direct method is also plotted in Figure 8A. Surprisingly, the CME-CELS method converges in fewer coefficient updates than the CME-direct method for $E > 15$.

Similar observations can be made by examining the total computational effort required for each method as a function of E (Figure 8B). The minimum computational effort required by SIMPLEC and UME-CELS is very close, whereas the minimum effort of the CME-CELS method

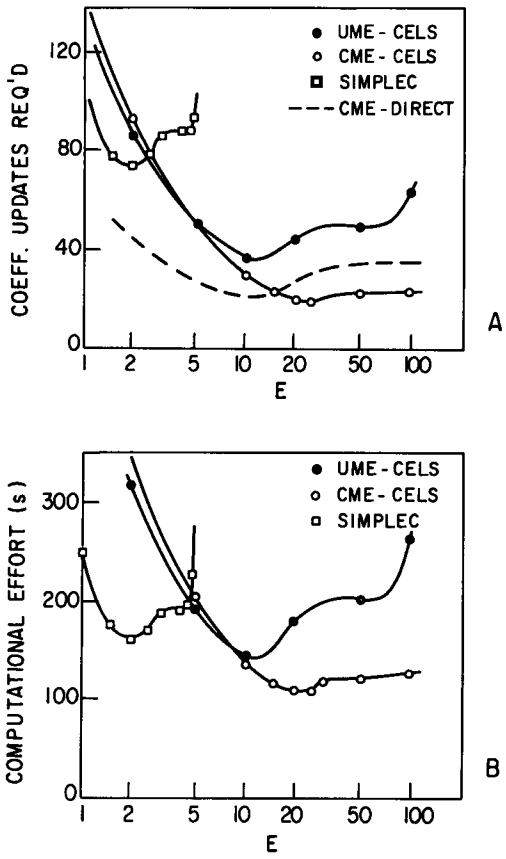

Figure 8. Convergence behaviour of the curvilinear test problem for various solution methods, measured in terms of the number of coefficient updates required (A), and the total computational effort required (B) for all variables to converge within $\varepsilon_{max} = 10^{-4}$ of their exact values versus the relaxation, E

is significantly less. The differences in total computational effort between CME-CELS and UME-CELS at large values of E are due solely to the difference in treatment of the non-linear terms. The computational efficiency of the CELS method, further enhanced by solving the momentum equations linearized as in the CME set, constitutes a robust, and economical solution procedure.

Summary of iterative solution results

The CELS method applied to the UME set results in a satisfactory treatment of the p–V coupling and results in a method which is competitive with SIMPLEC, a state-of-the-art segregated method. This is consistent with the conclusions of a previous study.[9] When CELS is extended to the solution of the equation set that embodies full Newton–Raphson linearization, the CME set, the performance is only slightly enhanced for the Cartesian problem. For the curvilinear problem, use of the CELS solution of the CME set results in substantial savings.

These findings are consistent with the results obtained for other test problems.

CONCLUSIONS

A study has been made to examine the degree of improvement of convergence rate that can be achieved using a Newton–Raphson linearization for all the non-linear terms in the general curvilinear equations of motion. A Newton–Raphson linearization for all the non-linear terms in the control-volume-based discrete momentum equations resulted in a coupled momentum equation set.

The CME set was solved using a direct linear solution procedure to isolate the effect of the treatment of the non-linear terms on the convergence to the steady-state solution. It was found that solving the CME set accelerates the convergence rate and at the same time is less sensitive to the major relaxation parameter used to optimize the convergence rate. The Newton–Raphson linearization of the acceleration terms arising in curvilinear co-ordinates was demonstrated to have an important effect on the convergence rate.

The CELS solution method was then extended to iteratively solve the proposed CME set. For the test problems analysed, the proposed combination of the Newton–Raphson linearizations and the CELS iterative linear solution method proved to be robust and computationally efficient, when compared to other current state-of-the-art solution methods.

ACKNOWLEDGEMENTS

The authors acknowledge the helpful discussions with J. P. Van Doormaal and other members of the Computational Fluid Dynamics Group at the University of Waterloo. Our special thanks also to L. N. Carlucci of Atomic Energy of Canada—CRNL for his interest, suggestions and support. The work was supported by Atomic Energy of Canada and the Natural Science and Engineering Research Council of Canada (NSERC).

NOMENCLATURE

$A_E^{c,u}$, $A_p^{u,v}$, etc.	coefficients of the discrete equations
A_e, A_w	areas of the control volume faces denoted by subscript
b	source term of a control volume applying along a given line
B	source term for a control volume
E	relaxation factor

h_1, h_2	metrics in the x_1 and x_2 directions
M	mass in a control volume
p	pressure
S_1	arc length in x_1 direction
$\dot{S}_u, \dot{S}_v$	source term in equation for variable denoted by subscript
t	time
u, v	velocity components in the x_1 and x_2 directions, respectively
V	velocity vector
Vol	volume of control volume
x_1, x_2	curvilinear co-ordinate directions

Greek

α	upwind weighting factor[13]
μ	viscosity of fluid
ρ	density of fluid
$\sigma_{11}, \sigma_{12}, \sigma$	curvilinear fluid stresses
ΔS	arc length increment
Δt	time increment

Subscripts

P, E, W, N, S	geographic node point location with respect to control volume of interest
e, w, n, s	geographic face point locations

Superscripts

o	denotes variables at the end of the previous time step or iteration
*	denotes most recent estimate of variable
c, u, v	denotes equation in which the coefficient applies
u, v, p	denotes the variable type which the coefficient multiplies

Acronyms

CELS	Iterative linear solution method based on a coupled equation line solver
CME	Coupled momentum equation set that arises from a full Newton–Raphson linearization
UME	Uncoupled momentum equation set that arises when the standard incompressible linearization is adopted

APPENDIX: LINEARIZED MOMENTUM EQUATION COEFFICIENTS

For completeness, the coefficients of the u-momentum equation are given below, where all the non-linear inertial terms have been approximated using a Newton–Raphson linearization. The coefficients of equation (8) are thus

$$A_P^{u,u} u_{ij} = A_E^{u,u} u_{i+1j} + A_W^{u,u} u_{i-1j} + A_N^{u,u} u_{ij-1} + A_S^{u,u} u_{ij-1} + A_{NE}^{u,v} v_{i+1j} + A_{NW}^{u,v} v_{ij} + A_{SE}^{u,v} v_{i+1j-1} + A_{SW}^{u,v} v_{ij-1} + A_E^{u,p} p_{i+1j} + A_W^{u,p} p_{ij} + B^{*u},$$

where

$$A_{\mathrm{E}}^{u,u} = -2\dot{m}_{\mathrm{e}}(\tfrac{1}{2} - \alpha_{\mathrm{e}}) + \mu\frac{A_{\mathrm{e}}}{\Delta S_{1\mathrm{e}}},$$

$$A_{\mathrm{W}}^{u,u} = +2\dot{m}_{\mathrm{w}}(\tfrac{1}{2} + \alpha_{\mathrm{w}}) + \mu\frac{A_{\mathrm{w}}}{\Delta S_{1\mathrm{w}}},$$

$$A_{\mathrm{N}}^{u,u} = -\dot{m}_{\mathrm{n}}(\tfrac{1}{2} - \alpha_{\mathrm{n}}) + \mu\frac{A_{\mathrm{n}}}{\Delta S_{2\mathrm{n}}},$$

$$A_{\mathrm{S}}^{u,u} = +\dot{m}_{\mathrm{s}}(\tfrac{1}{2} + \alpha_{\mathrm{s}}) + \mu\frac{A_{\mathrm{s}}}{\Delta S_{2\mathrm{s}}},$$

$$A_{\mathrm{NE}}^{u,v} = -\tfrac{1}{2}\rho A_{\mathrm{NE}}u_{\mathrm{n}}^0 + C_3, \quad A_{\mathrm{NW}}^{u,v} = -\tfrac{1}{2}\rho A_{\mathrm{NW}}u_{\mathrm{n}}^0 + C_3,$$

$$A_{\mathrm{SE}}^{u,v} = +\tfrac{1}{2}\rho A_{\mathrm{SE}}u_{\mathrm{s}}^0 + C_3, \quad A_{\mathrm{SW}}^{u,v} = +\tfrac{1}{2}\rho A_{\mathrm{SW}}u_{\mathrm{s}}^0 + C_3,$$

$$B^{*u} = B^u + \dot{m}_{\mathrm{e}}u_{\mathrm{e}}^0 - \dot{m}_{\mathrm{w}}u_{\mathrm{w}}^0 + \dot{m}_{\mathrm{n}}u_{\mathrm{n}}^0 - \dot{m}_{\mathrm{s}}u_{\mathrm{s}}^0 + C_1u_{\mathrm{p}}^0v_{\mathrm{P}}^{u^0} - C_2v_{\mathrm{P}}^{u^02} + \left[\frac{\Sigma A_{\mathrm{nb}}^{u,u}}{E} - \min(C_1v_{\mathrm{P}}^{u^0}, 0)\right]u_{\mathrm{p}}^0$$

$$A_{\mathrm{p}}^{u,u} = \Sigma A_{\mathrm{nb}}^{u,u}\left(1 + \frac{1}{E}\right) + \dot{m}_{\mathrm{e}}(\tfrac{1}{2} + \alpha_{\mathrm{e}}) - \dot{m}_{\mathrm{w}}(\tfrac{1}{2} - \alpha_{\mathrm{w}}) + \max(C_1v_{\mathrm{P}}^{u^0}, 0)$$

$$\Sigma A_{\mathrm{nb}}^{u,u} = A_{\mathrm{E}}^{u,u} + A_{\mathrm{W}}^{u,u} + A_{\mathrm{N}}^{u,u} + A_{\mathrm{S}}^{u,u} + \dot{m}_{\mathrm{e}}(\tfrac{1}{2} - \alpha_{\mathrm{e}}) - \dot{m}_{\mathrm{w}}(\tfrac{1}{2} + \alpha_{\mathrm{w}})$$

$$C_1 = \rho(A_{\mathrm{n}} - A_{\mathrm{s}})$$

$$C_2 = \rho(A_{\mathrm{e}} - A_{\mathrm{w}})$$

$$C_3 = -\frac{C_1}{4}u_{\mathrm{P}}^0 + \frac{C_2}{2}v_{\mathrm{P}}^{u^0}$$

$$v_{\mathrm{P}}^{u^0} = \tfrac{1}{4}(v_{i+1j}^0 + v_{ij}^0 + v_{i+1j-1}^0 + v_{ij-1}^0)$$

$$A_{\mathrm{W}}^{u,p} = -A_{\mathrm{E}}^{u,p} = \frac{\mathrm{Vol}}{\Delta S_{1\mathrm{p}}}$$

The v-momentum equation coefficients are exactly analogous to the u-momentum equation coefficients above. Complete details of the general orthogonal discrete method are available in Reference 12.

REFERENCES

1. R. M. Beam and R. F. Warming, 'An implicit finite difference algorithm for hyperbolic systems in conservation-law form', *J. Comp. Physics*, **22**, 87–110 (1976).
2. R. M. Beam and R. F. Warming, 'An implicit factored scheme for the compressible Navier–Stokes equations', presented at the *AIAA 3rd Computational Fluid Dynamics Conference*, Albuquerque, NM, 1977.
3. W. R. Briley and H. McDonald, 'Solution of the multidimensional compressible Navier–Stokes equations by a generalized implicit method', *J. Comp. Physics*, **24**, 372–397 (1977).
4. W. R. Briley and H. McDonald, 'On the structure and use of linearized block implicit schemes', *J. Comp. Physics*, **34**, 54–73 (1980).
5. R. W. MacCormick, 'Current status of numerical solutions of the Navier–Stokes equations', presented at the *AIAA 23rd Aerospace Sciences Meeting*, 1985.
6. S. V. Patankar, '*Numerical Heat Transfer and Fluid Flow*, Hemisphere, New York, 1980.

7. J. P. Van Doormaal and G. D. Raithby, 'Enhancements of the SIMPLE method for predicting incompressible fluid flows', *Numer. Heat Transfer*, **7**, 147–163 (1984).
8. J. P. Van Doormaal and G. D. Raithby, 'The simultaneous solution along lines of the continuity and momentum equations', *IMACS Conference*, Montreal, 1982.
9. P. F. Galpin, J. P. Van Doormaal and G. D. Raithby, 'Solution of the incompressible mass and momentum equations by application of a coupled equation line solver', *Int. j. numer. methods fluids* **5**, 615–625 (1985).
10. W. F. Hughes and E. W. Gaylord, *Basic Equations of Engineering Science*, Schaum's Outline Series, McGraw Hill, New York, 1964.
11. F. H. Harlow and J. E. Welch, 'Numerical calculation of time-dependent viscous incompressible flow of fluid with free surface', *Physics of Fluids*, **8**, 2182–2189 (1965).
12. G. D. Raithby, P. F. Galpin and J. P. Van Doormaal, 'Prediction of heat and fluid flow in complex geometries using general orthogonal coordinates', *Numer. Heat Transfer*, **9**, 125–142 (1986).
13. G. D. Raithby and K. E. Torrance, 'Upstream weighted differencing schemes and their application to elliptic problems involving fluid flow', *Computers and Fluids*, **2**, 191–206 (1974).
14. G. D. Raithby and G. E. Schneider, 'Numerical solution of problems in incompressible fluid flow; treatment of the velocity–pressure coupling', *Numer. Heat Transfer*, **2**, 417–440 (1979).
15. M. Zedan and G. E. Schneider, 'A strongly implicit simultaneous variable solution procedure for velocity and pressure in fluid flow problems', *AIAA 18th Thermophysics Conference*, Montreal, 1983.
16. M. Zedan and G. E. Schneider, 'Investigation of the simultaneous variable solution procedure for velocity and pressure in fluid flow problems', *AIAA 18th Thermophysics Conference*, Montreal, 1983.
17. P. F. Galpin, *M.A.Sc. thesis, Dept. of Mechanical Engineering*, University of Waterloo, Waterloo, Ontario, (1985).